Photonic Network Communications
https://doi.org/10.1007/s11107-020-00917-5

ORIGINAL PAPER

Ultra-fast all-optical full-adder based on nonlinear photonic crystal resonant cavities

M. J. Maleki[1] · A. Mir[1] · M. Soroosh[2]

Received: 26 October 2019 / Accepted: 12 October 2020

Abstract
In this paper, a new photonic crystal-based full-adder for the summation of three bits has been proposed. For realizing this device, three input waveguides are connected to the main waveguide. An optical power splitter is placed at the end of this waveguide. Concerning the amount of optical intensity inside this waveguide, two nonlinear resonant cavities transmit the waves toward the correct ports. When the cavities do not drop the optical waves, the splitter guides them toward the output ports. The maximum delay time of the presented structure is around 0.5 ps and shows the fastest response among the reported works. This improvement is obtained due to using the resonant cavities. The time analysis results in a maximum working frequency of 2 THz. Also, designing the structure in 93 μm^2 demonstrates that it is more compact than the previous works. The normalized low and high margins are obtained around 10% and 85%, respectively. So, the proposed device is capable of considering optical processing circuits.

Keywords Full-adder · Kerr effect · Photonic bandgap · Photonic crystal · Resonant cavity

1 Introduction

Due to increasing demands for wide bandwidth and ultra-fast processing, many attempts have been made to design and develop the optical processing systems. One of the essential components in digital circuits is the full-adder. This device sums three bits and generates two output bits, sum and carry. The main challenge in designing n-bit full-adders is the latency of developing the carry bit for the next stages. The electrical full-adders suffer the mentioned latency when the number of bits is increased. Different ideas such as generating carry signals in the form of the optical waves [1] and designing plasmonic-based [2] and photonic crystal-based [3–7] structures have been proposed to overcome this challenge.

Ying et al. [1] proposed an electro-optical modulator for generating the carry in optical waves. They used a continuous wave and modulated it as the optical carry for the next stages. Although the electric signals modulate the carry, the output optical signal should be converted to the electric form. This issue has not been considered in their work. Concerning the reported time for the electro-optical modulators (50 ps), it seems that this idea will not be applicable to design the ultra-fast processors. Xie et al. [2] designed and fabricated the cross-connected plasmonic waveguides to utilize the all-optical full-adder. Two plasmonic nano-cavities were side-coupled with the output waveguides. These cavities were covered with high-nonlinear coefficient nanocomposite layers. The plasmonic-based full-adder working states obtained correspond to the different modes, while the single-mode designing is preferred for operation. Although the time analysis was not reported, the all-optical processing can improve the time-consuming compared to the previous work [1].

Photonic crystals (PhCs) [8, 9] are known as the proper structures for designing all-optical devices. They are the periodic arrangement of dielectric materials that propagate and manipulate the light flow in the desired waveguides. The wavelength should be inside the photonic bandgap (PBG) of the structure to confine the waveguide's optical waves. Scalability, small size, and no need for electrical bias are the main advantages of PhC-based devices [10–14]. In recent years, several PhC-based devices such as optical

✉ M. Soroosh
m.soroosh@scu.ac.ir

[1] Faculty of Engineering, Lorestan University, Khorramabad, Iran

[2] Department of Electrical Engineering, Shahid Chamran University of Ahvaz, Ahvaz, Iran

Published online: 31 October 2020

filters [15–22], demultiplexers [23–29], logic gates [30–38], decoders [39–43], encoders [44–48], and analog-to-digital converters [49–54] have been proposed.

Alipour-Banaei and Seif-Dargahi [3] proposed a photonic crystal-based optical full-adder. The proposed structure was realized by cascading two optical half-adders. In this study, two nonlinear ring resonators with similar optical characteristics were used. Although they reported the rise time of 2 ps, the designed structure area was as large as 439 μm^2. Cheraghi et al. proposed another PhC-based full-adder in which the dropping of optical waves occurred concerning the amount of optical intensity [4]. They used four nonlinear resonant cavities in a two-dimensional square lattice for guiding the waves toward the desired output ports [4]. Although the area was reduced to 396 μm^2 compared to the previous work [3], the rise time of 8 ps was obtained. Swarnakar et al. [5] designed a structure based on the cross-connected waveguides and used the inputs with different phases. They succeeded in reducing the rise time to 1 ps compared to the previous works. Moradi et al. [6] have designed a square arrangement of rods, including two ring resonators. They improved the difference of margins; however, the rise time was increased to 3 ps. Recently, Vali-Nasab et al. [7] have proposed a structure including two cross-connected waveguides for both output ports. They placed two nonlinear rods at the cross-connections to make the desired interferences. The small size around 72 μm^2 and the rise time of 2 ps are the main advantages of this structure.

Considering the structures mentioned above for optical full-adders demonstrates that designing the ultra-fast structures is an attractive challenge for researchers. In this paper, concerning the presented idea by Cheraghi et al. [4], we will propose an ultra-fast and compact structure for all-optical full-adder. The structure includes two nonlinear resonant cavities. Incoming optical signals from the inputs are combined and transmitted to the main waveguide. Concerning the amount of the optical intensity in the main waveguide, two resonant cavities guide the waves toward the desired output ports. Cheraghi et al. used two resonant cavities at the end of the main waveguide for dropping the waves to the state that all input bits were equal to 1 [4]. Although these cavities assisted in obtaining the correct operation, the reflected waves interfered with the traveling ones in the main waveguide for other states. This issue resulted in increasing the rise time and decreasing the margin of logic 1. In this study, a beam splitter has been placed at the end of the main waveguide to divide the optical signal into two equal parts. Each part activates one of the output ports when all input ports are at logic 1. The less portion of the reflected waves affects the traveling waves in the main waveguide for other states. For improving the wave dropping from the main waveguide to the cavities, the radii of the first rods at the cavities were tuned at 84 nm. Therefore, the proposed structure's rise time was improved to 0.5 ps compared to all previous works.

Concerning the lattice constant of 475 nm and the radius of 105 nm, the structure's footprint was also improved. Besides, this work includes a more considerable difference between the mentioned margins than one for Refs [3–5, 7]. In Sect. 2, the design procedure of the proposed structure will be introduced. Then, the simulation results will be shown and compared to ones for other works, in Sect. 3. The conclusion of this work will be presented in Sect. 4.

2 Design procedure

A square lattice of dielectric rods with the air gaps, including 18 rows and 23 columns along the x and z directions, is used as the two-dimensional fundamental structure. The refractive index and radius of the dielectric rods are 3.1 and 0.22a, respectively, where $a = 475$ nm is the lattice constant. According to Bragg's theory, this assumption helps obtain a large PBG for the proposed structure [55]. The plane wave expansion method was used to calculate the band diagram [56]. In Maxwell's equations, electric (E) and magnetic (H) fields could be described in the Fourier's series because of the periodic rods. So, $\left(\frac{\omega}{c}\right)^2$ as the eigenvalue of $\frac{1}{\varepsilon_r}\nabla\times\nabla\times E = \left(\frac{\omega}{c}\right)^2 E$ and $\nabla\times\frac{1}{\varepsilon_r}\nabla\times H = \left(\frac{\omega}{c}\right)^2 H$ equations was calculated for the different wave vectors [2]. ω is the frequency, c is the light velocity in the vacuum, and ε is the dielectric constant. The band diagram and the Brillouin zone of the PhC structure are shown in Fig. 1. One can see the presented lattice includes a PBG (blue hatched area) in TM mode. Concerning $a = 475$ nm, this gap covers the range of 1131–1638 nm. The obtained wide range is advantageous to the structure and covers the optical communication bands such as C and L [57].

For realizing the proposed full-adder structure, three waveguides (W1, W2, and W3) are connected to three input ports A, B, and C, respectively (Fig. 2). The launched signals from A, B, and C ports are guided toward W5 waveguide through W1, W2, W3, and W4. Two resonant cavities (C1 and C2), including nonlinear rods, are located on both sides of W5 for making the dropping operation concerning the amount of optical intensity inside W5.

In this structure, two nonlinear rods (with green and blue colors) have been used in both cavities. The green rod is made of a doped glass with a linear refractive index and an optical Kerr coefficient of 1.4 and 10–14 m2/W, respectively [53]. Another nonlinear rod is made of the chalcogenide with a linear refractive index of 3.1 and an optical Kerr coefficient of 9×10^{-17} m^2/W [58]. The radii of the rods are shown in Fig. 2.

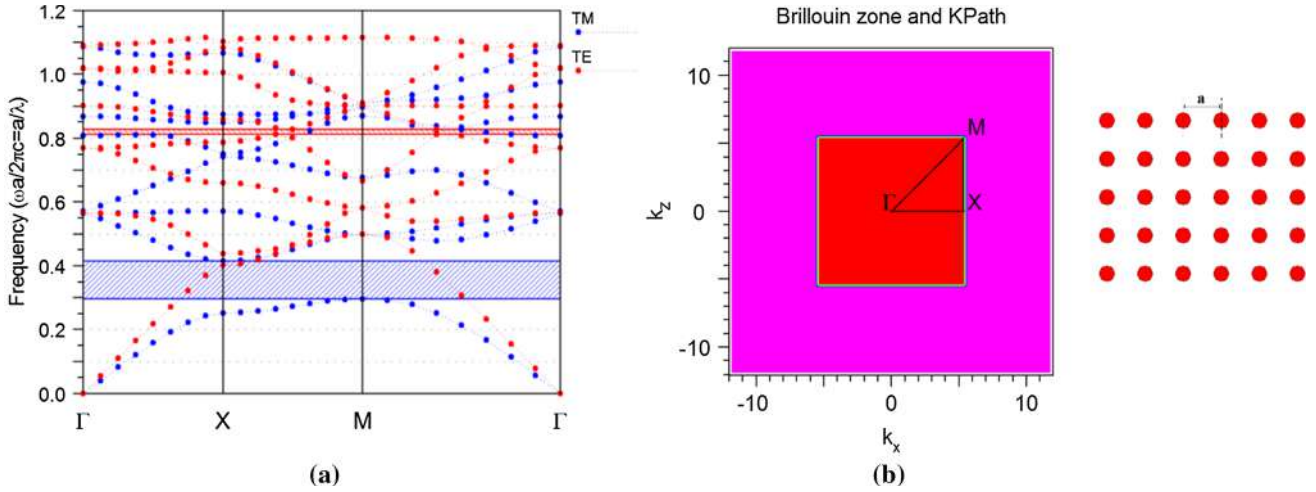

Fig. 1 **a** The calculated band diagram, **b** the Brillouin zone of the structure at *x* and *z* directions. The red disks present a top view of the rods (Color figure online)

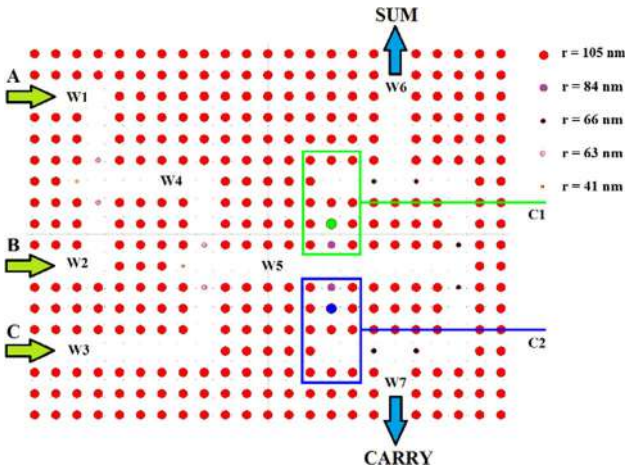

Fig. 2 The proposed structure for full-adder

Table 1 Working states of the structure

Input states			Light intensity inside W5	Logic for output ports	
A	B	C		SUM	CARRY
0	0	0	–	0	0
0	0	1	I0	1	0
0	1	0	I0	1	0
0	1	1	2I0	0	1
1	0	0	I0	1	0
1	0	1	2I0	0	1
1	1	0	2I0	0	1
1	1	1	3I0	1	1

The refractive index of nonlinear rods (n) is changed according to the incident optical intensity (I). This issue is known as the optical Kerr effect and is defined by $n = n_0 + kI$, where n_0 is the linear refractive index and k is the nonlinear coefficient [59, 60]. The resonant wavelength of both cavities depends on the refractive index of the nonlinear rods. Also, the amount of the optical intensity inside W5 is changed for the different states of inputs. By tuning the radii of nonlinear rods, the optical waves will be transmitted from W5 to W6 and W7 waveguides when the optical intensity is equal to I0 and 2I0, respectively. I0 shows the value of optical intensity inside W5 when one of the input ports is active. In this state, C1 cavity couples the waves to W6, so SUM port is activated.

When two input ports are at logic, the optical intensity inside W5 is equal to 2I0. So, the optical signals are coupled to W7 through C2 cavity, and CARRY port is activated. If all input ports are at logic 1, the amount of the optical intensity inside W5 is equal to 3I0, so the waves reach the end of W5 waveguide. At the end of W5, a splitter has been placed to guide the optical waves toward SUM and CARRY ports. In this state, both output ports are activated. The working states are summarized in Table 1.

Concerning the lattice constant and the radius of rods, the area is just around 93 μm^2, so it is more compact than other structures [3–6].

3 Simulation and results

The finite difference time domain (FDTD) method is used to simulate the optical wave propagation throughout the structure. In this method, Maxwell's equations are discretized in space and time. Based on Yee's cell, the electric and magnetic fields at each cell are calculated using the four

neighboring cells [61]. The structure is discretized in space by $\Delta x = \Delta z = 10$ nm in which the length of the unit cell is smaller than $\lambda/10$ where λ is the wavelength. Three optical waves with a central wavelength of 1550 nm and an optical intensity of 100 mW/μm^2 are used for the input signals. According to the Courant condition, the time step of 10 is used for the time step [61].

Because the structure includes three input ports, eight different working states are possible that should be considered. Figure 3 shows the distribution of the normalized optical fields inside the proposed structure. Furthermore, the pulse response has been calculated for all possible states, as shown in Fig. 4. The duration time of the pulse is 9 ps. Figure 4 shows that the normalized power at the output port is defined as the amount of optical power at the output port divided by the input power at one port. So, the normalized value can be more than one if two or three input ports are activated. In this study, the maximum amount of the rise and fall times is known as a delay. The rise time is defined as the time that the signal goes up to reach 90% of the steady-state value.

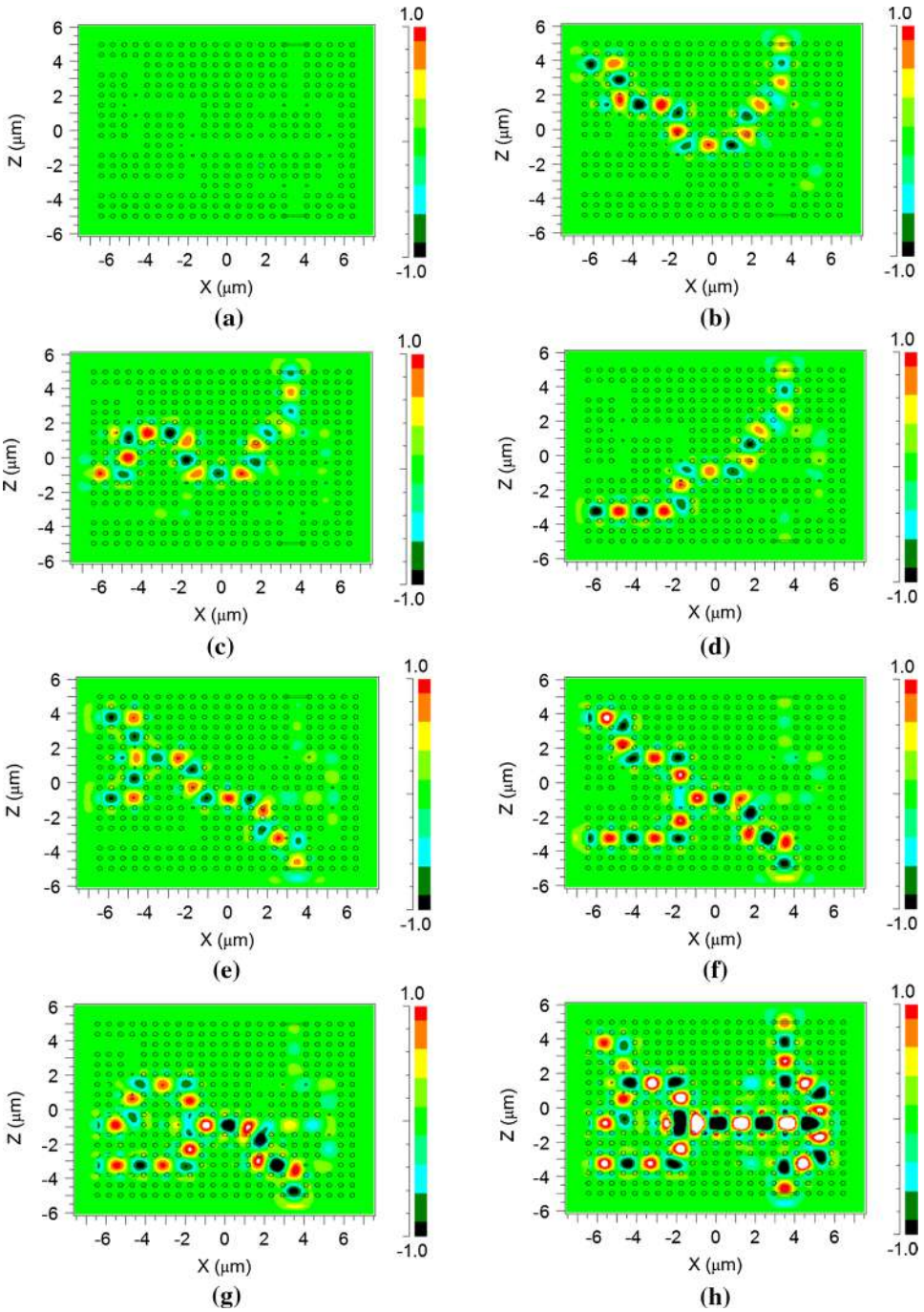

Fig. 3 Optical wave propagation inside the proposed structure for all working states; **a** $ABC = 000$, **b** $ABC = 100$, **c** $ABC = 010$, **d** $ABC = 001$, **e** $ABC = 110$, **f** $ABC = 101$, **g** $ABC = 011$, **h** $ABC = 111$

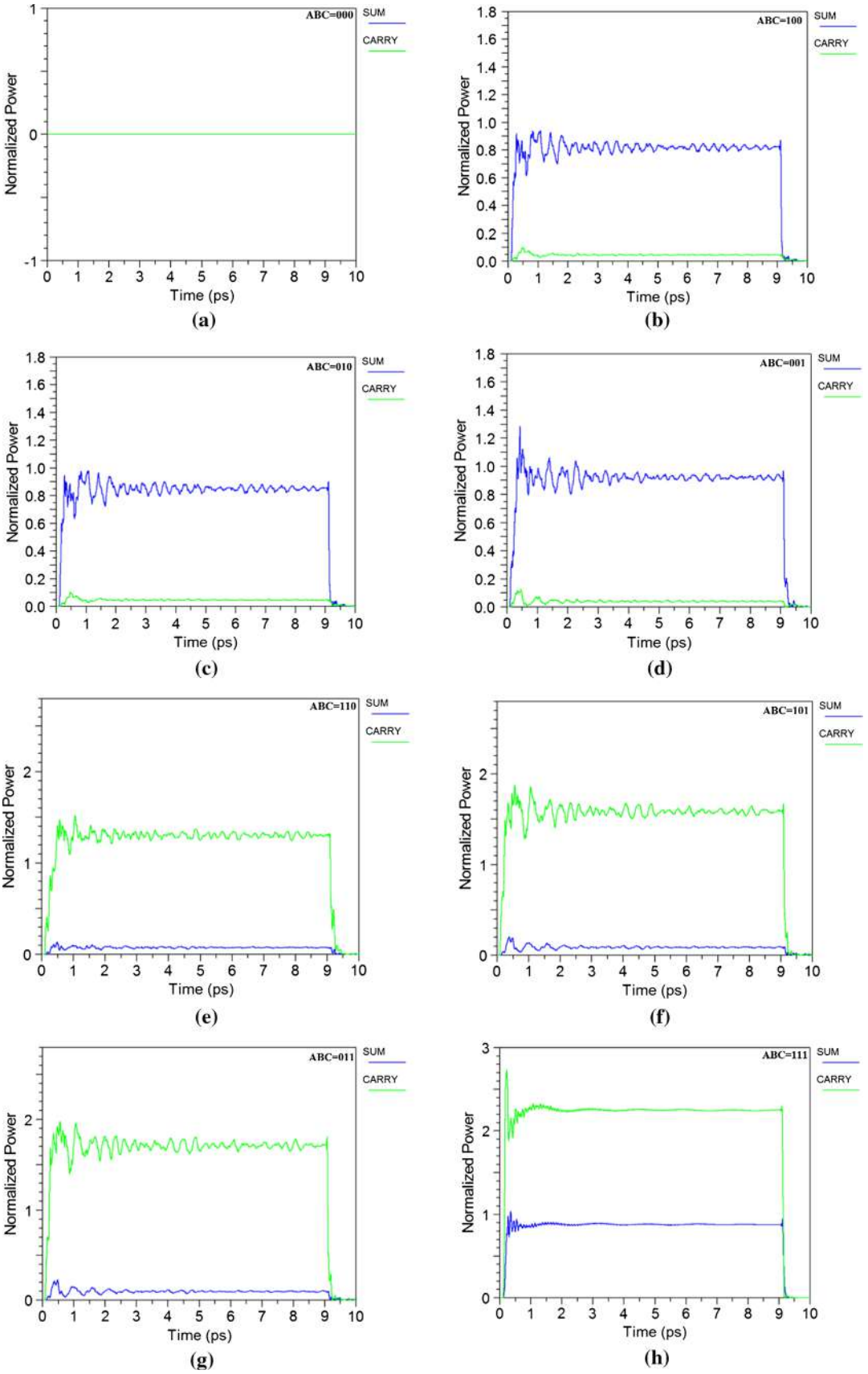

Fig. 4 Time response for different states; **a** $ABC = 000$, **b** $ABC = 100$, **c** $ABC = 010$, **d** $ABC = 001$, **e** $ABC = 110$, **f** ABC = 101, **g** $ABC = 011$, **h** $ABC = 111$

The fall time is also defined as the needed time to decrease 10% of the initial value.

It is evident that when the input ports are inactive, there is no optical wave inside the structure, so the output ports are assumed at logic 0 (Figs. 3a and 4a). As shown in Fig. 3b, c, and d, when the optical waves are applied to one of the input ports (i.e., $A=1$, $B=C=0$, or $B=1$, $A=C=0$, or $C=1$, $A=B=0$), C1 cavity drops them to W6 waveguide. Therefore, the minimum amount of the normalized optical intensities at SUM port and the maximum one at CARRY port are equal to 85% and 4%, respectively. As a result, SUM and CARRY ports are at logics 1 and 0, respectively. For these states, the maximum delay time is around 0.41 ps, and the time response diagrams are shown in Fig. 4b, c, and d.

When the optical waves are applied to two input ports (i.e., $A=B=1$, $C=0$ or $A=C=1$, $B=0$ or $B=C=1$, $A=0$), C2 cavity guides the waves to W7 waveguide and CARRY port is activated. Figure 3e, f, and g shows the optical wave propagation inside the structure when one input port is inactive. The time analysis of these states demonstrates the maximum amount of the normalized optical intensities at SUM port, and the minimum one at CARRY port are 10% and 134%, respectively (Fig. 4e, f, and g). Also, the maximum delay time of 0.46 ps is obtained for these states.

Finally, if the optical waves are applied to all input ports ($A=B=C=1$), the cavities do not drop them to W6 and W7, so they reach the splitter and activate the output ports (Fig. 3h). In this state, the amount of the normalized optical intensities at SUM and CARRY ports are equal to 88% and 225%, respectively (Fig. 4h). So, the output ports are assumed at logic 1. The delay time of this state is around 0.5 ps.

Figure 5 shows the normalized power in the cavities versus the optical intensity inside W5 waveguide. It can be seen that the maximum droppings through C1 and C2 cavities occur for I0 and 2I0, respectively, where I0 is equal to 0.1 W/μm^2. According to Bragg's theory, the reflected waves from the periodic bilayers are in phase if the equation $n_1d_1+n_2d_2=\lambda/2$ is satisfied [62]. n_1 and n_2 are the refractive indices, and d_1 and d_2 are the thicknesses of the layers. So, using the different radii in cavities, the dropping operation for I0 and 2I0 is possible.

The performance of the proposed structure for all working states is summarized in Table 2. Comparing the calculated table to the truth table of a typical full-adder confirms the proposed structure's correct operation. Based on the obtained results, the minimum value of the normalized intensity at output ports for logic 1 is 85%. Also, the maximum amount of the intensity for logic 0 is 10%. These values are the worst cases to determine the logic margins of the structure. Therefore, 10% and 85% can be assumed as the margins of logics 0 and 1, respectively.

The contrast ratio is defined by $10\times\log(M1/M0)$, where M1 and M0 are the margins for logics 1 and 0, respectively [7]. Concerning $M1=85\%$ and $M0=10\%$, the contrast ratio is equal to 9.3 dB. Bit rate refers to the speed at which the data are transferred and is defined by $1/T_{ss}$ where T_{ss} is the steady-state time. The steady-state time is defined as when the variation of the signal is confined to 5% of the final value. So, the bit rate of the structure is around 0.2 THz.

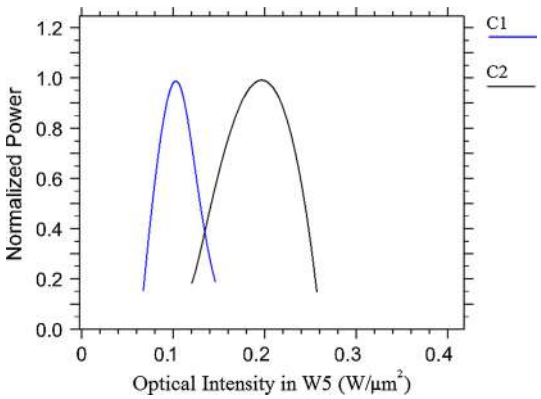

Fig. 5 Normalized power in the cavities versus the optical intensity in W5

Table 2 Simulation results for different input states

Input states			Output ports				Rise time (ps)	Fall time (ps)
			Logic		Normalized intensity (%)			
A	B	C	SUM	CARRY	SUM	CARRY		
0	0	0	0	0	0	0	–	–
0	0	1	1	0	94	4	0.39	0.21
0	1	0	1	0	86	4	0.41	0.26
0	1	1	0	1	10	176	0.44	0.23
1	0	0	1	0	85	4	0.4	0.24
1	0	1	0	1	8	165	0.42	0.27
1	1	0	0	1	8	134	0.46	0.32
1	1	1	1	1	88	225	0.5	0.27

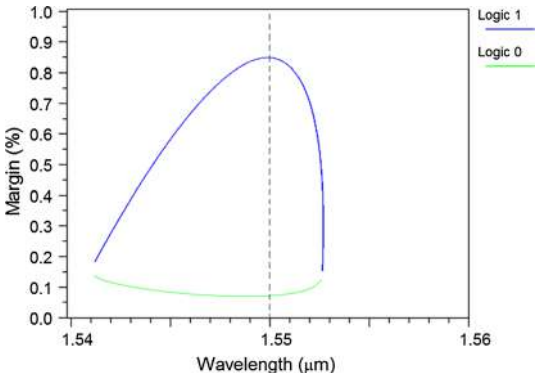

Fig. 6 The calculated margins of the structure for the different wavelengths

Table 3 Comparison of the obtained results with other works

Work	Area (μm^2)	T_d (ps)	DM (%)
[48]	439	2	55
[49]	396	8	43
[50]	346	1	28
[51]	560	3	81
[52]	72	2	60
This work	93	0.5	75

Figure 6 shows the margin of logics versus the wavelength. All possible states were considered for each wavelength, and the margins of logics 0 and 1 were calculated. It can be seen that the maximum contrast ratio is obtained at the wavelength of 1550 nm. Also, there is a gap between the margins for the range of 1541–1552 nm. This structure has been designed for the wavelength of 1550 nm, so for another wavelength, the radii of defect rods should be changed.

To additional assessment, a comparison of the proposed full-adder with other works is given in Table 3. Area, delay time (T_d), and the difference between margins for logics 0 and 1 (DM) as the essential parameters are investigated for this work and Refs [3–7]. The small size of the presented structure is advantageous for this work and is a proper result for optical integrated circuits. The compactness of the structure results in decreasing the delay time. One can see that the obtained delay time has been reduced to 0.5 ps compared to Refs [3–7]. Concerning the value of 0.5 ps, the maximum working frequency of 2 THz is obtained for the proposed device. Concerning the increasing demands for ultra-fast processing, this improvement can be considered an essential advantage in designing all-optical full-adder. The last column of Table 3 presents the difference in margins for logics 0 and 1. It can be seen that the calculated value is more than one reported in Refs [3–5, 7]. Consequently, the presented all-optical full-adder can be potentially considered as a proper candidate for optical integrated circuits.

Many attempts have been done for the fabrication of photonic crystal-based structures [63–72]. They have used different methods to fabricate these structures, such as colloidal self-assembly, electron beam lithography, and direct writing via multiphoton microlithography. Deviation of the rods respect to the vertical axis, the ruggedness of rods, and the non-periodicity of the lattice are the main challenges of the fabrication process. Concerning these researches, they have been succeeded in decreasing the radius of rods to 40 nm. The smallest radius of rods in the presented structure is equal to 41 nm. So, one can be optimistic about fabricating the proposed device.

4 Conclusion

In this paper, a new photonic crystal-based structure for realizing an all-optical full-adder was proposed. Input signals were guided to the main waveguide through four waveguides. Two resonant cavities including nonlinear rods and one splitter transmitted optical waves toward the output ports. The simulation of the optical wave propagation for eight possible states demonstrated the correct operation of the structure. Small size and fast response of the presented device compared to other works were the main advantages of this work. The simulation results showed that the area and the delay time of the proposed full-adder were around 93 μm^2 and 0.5 ps, respectively. Furthermore, the amount of 10% and 85% was obtained as the margins for logics 0 and 1, respectively. Based on the simulation results, the presented all-optical full-adder can be considered for optical integrated circuits.

References

1. Ying, Z., Wang, Z., Zhao, Z., Dhar, S., Pan, D.Z., Soref, R., Chen, R.T.: Silicon microdisk-based full adders for optical computing. Opt Lett **43**, 983–986 (2018)
2. Xiea, J., Niua, X., Hu, X., Wang, F., Chai, Z., Yang, H., Gong, Q.: Ultracompact all-optical full-adder and half-adder based on nonlinear plasmonic nanocavities. Nanophotonics **6**, 1161–1173 (2017)
3. Alipour-Banaei, H., Seif-Dargahi, H.: Photonic crystal based 1-bit full-adder optical circuit by using ring resonators in a nonlinear structure. Photonics Nanostruct Fundam Appl. **24**, 29–34 (2017)
4. Cheraghi, F., Soroosh, M., Akbarizadeh, G.: An ultra-compact all optical full-adder based on nonlinear photonic crystal resonant cavities. Superlattices Microstruct. **28**, 154–161 (2018)
5. Swarnakar, S., Kumar, S., Sharma, S.: Performance analysis of all-optical full-adder based on two-dimensional photonic crystals. J. Comp. Electron. **43**, 47–53 (2019)

6. Moradi, M., Danaie, M., Orouji, A.A.: Design and analysis of an optical full-adder based on nonlinear photonic crystal ring resonators. Opt. Int. J. Light Electron Opt. **172**, 127–136 (2018)
7. Vali-Nasab, A.M., Mir, A., Talebzadeh, R.: Design and simulation of an all optical full-adder based on photonic crystals. Opt. Quant. Electron. **51**, 161 (2019)
8. John, S.: Strong localization of photons in certain disordered dielectric superlattices. Phys. Rev. Lett. **58**, 2486–2489 (1987)
9. Yablonovitch, E.: Inhibited spontaneous emission in solid-state physics and electronics. Phys. Rev. Lett. **58**, 2059–2062 (1987)
10. Mehdizadeh, F., Alipour-Banaei, H.: Bandgap management in two-dimensional photonic crystal thue-morse structures. J. Opt. Commun. **34**, 61–65 (2013)
11. Alipour-Banaei, H., Mehdizadeh, F.: Bandgap calculation of 2D hexagonal photonic crystal structures based on regression analysis. J. Opt. Commun. **34**, 1–9 (2013)
12. Liu, D., Gao, Y., Tong, A., Hu, S.: Absolute photonic band gap in 2D honeycomb annular photonic crystals. Phys. Lett. A. **379**, 214–217 (2015)
13. M. Reza Rakhshani, Ali Mansouri-Birjandi M.: Design and simulation of wavelength demultiplexer based on heterostructure photonic crystals ring resonators. Phys. E Low-Dimensional Syst. Nanostruct. **50**, 97–101 (2013)
14. Djavid, M., Monifi, F., Ghaffari, A., Abrishamian, M.S.: Heterostructure wavelength division demultiplexers using photonic crystal ring resonators. Opt. Commun. **281**, 4028–4032 (2008)
15. Musavizadeh, S.M., Soroosh, M., Mehdizadeh, F.: Optical filter based on photonic crystal. Indian J. Pure Appl. Phys. **53**, 736–739 (2015)
16. Dideban, A., Habibiyan, H., Ghafoorifard, H.: Photonic crystal channel drop filter based on ring-shaped defects for DWDM systems. Phys. E Low-Dimensional Syst. Nanostructures. **87**, 77–83 (2017)
17. Mansouri-Birjandi, M.A., Tavousi, A., Ghadrdan, M.: Full-optical tunable add/drop filter based on nonlinear photonic crystal ring resonators. Photonics Nanostructures Fundam. Appl. **21**, 44–51 (2016)
18. Tavousi, A., Mansouri-Birjandi, M.A., Ghadrdan, M., Ranjbar-Torkamani, M.: Application of photonic crystal ring resonator nonlinear response for full-optical tunable add–drop filtering. Photonic Netw. Commun. **34**, 131–139 (2017)
19. Zavvari, M., Mehdizadeh, F.: Photonic crystal cavity with L3-defect for resonant optical filtering. Frequenz. **68**, 519–523 (2014)
20. Qiang, Z., Zhou, W., Soref, R.a.: Optical add-drop filters based on photonic crystal ring resonators. Opt. Express. **15**, 1823–1831 (2007)
21. Youcef Mahmoud, M., Bassou, G., Taalbi, A., Chekroun, Z.M.: Optical channel drop filters based on photonic crystal ring resonators. Opt. Commun. **285**, 368–372 (2012)
22. Youcef Mahmoud, M., Bassou, G., Taalbi, A.: A new optical add–drop filter based on two-dimensional photonic crystal ring resonator. Opt. Int. J. Light Electron Opt. **124**(2013), 2864–2867 (2013)
23. Venkatachalam, K., Kumar, D.S., Robinson, S.: Investigation on 2D photonic crystal-based eight-channel wavelength-division demultiplexer. Photonic Netw. Commun. **34**, 63–68 (2017)
24. Kannaiyan, V., Savarimuthu, R., Dhamodharan, S.K.: Performance analysis of an eight channel demultiplexer using a 2D-photonic crystal quasi square ring resonator. Opto-Electronics Rev. **25**, 74–79 (2017)
25. Talebzadeh, R., Soroosh, M., Kavian, Y.S., Mehdizadeh, F.: Eight-channel all-optical demultiplexer based on photonic crystal resonant cavities. Opt. Int. J. Light Electron Opt. **140**, 331–337 (2017)
26. Fallahi, V., Seifouri, M., Olyaee, S., Alipour-Banaei, H.: Four-channel optical demultiplexer based on hexagonal photonic crystal ring resonators. Opt. Rev. **24**(2017), 605–610 (2017)
27. Mehdizadeh, F., Soroosh, M.: A new proposal for eight-channel optical demultiplexer based on photonic crystal resonant cavities. Photonic Netw. Commun. **31**, 65–70 (2016a)
28. Mehdizadeh, F., Soroosh, M., Alipour-Banaei, H.: An optical demultiplexer based on photonic crystal ring resonators. Opt. Int. J. Light Electron Opt. **127**, 8706–8709 (2016)
29. Alipour-Banaei, H., Serajmohammadi, S., Mehdizadeh, F.: Optical wavelength demultiplexer based on photonic crystal ring resonators. Photonic Netw. Commun. **29**, 146–150 (2014)
30. Mehdizadeh, F., Soroosh, M.: Designing of all optical NOR gate based on photonic crystal. Indian J. Pure Appl. Phys. **54**, 35–39 (2016b)
31. N. M. D'souza, V. Mathew, : Interference based square lattice photonic crystal logic gates working with different wavelengths. Opt. Laser Technol. **80**, 214–219 (2016)
32. Christina, X.S., Kabilan, A.P.: Design of optical logic gates using self-collimated beams in 2D photonic crystal. Photonic Sensors. **2**, 173–179 (2012)
33. Rani, P., Kalra, Y., Sinha, R.K.: Design and analysis of polarization independent all-optical logic gates in silicon-on-insulator photonic crystal. Opt. Commun. **374**, 148–155 (2016)
34. Rani, P., Kalra, Y., Sinha, R.K.: Realization of and gate in y shaped photonic crystal waveguide. Opt. Commun. **298–299**, 227–231 (2013)
35. Alipour-Banaei, H., Serajmohammadi, S., Mehdizadeh, F.: All optical NAND gate based on nonlinear photonic crystal ring resonators. Opt. Int. J. Light Electron Opt. **130**, 1214–1221 (2017)
36. Bao, J., Xiao, J., Fan, L., Li, X., Hai, Y., Zhang, T., et al.: All-optical NOR and NAND gates based on photonic crystal ring resonator. Opt. Commun. **329**, 109–112 (2014)
37. Wu, K.S., Dong, J.W., Chen, D.H., Luo, X.N., Wang, H.Z.: Sensitive photonic crystal phase logic gates. J. Mod. Opt. **56**, 1895–1898 (2009)
38. Mohebbi, Z., Nozhat, N., Emami, F.: High contrast all-optical logic gates based on 2D nonlinear photonic crystal. Opt. Commun. **355**, 130–136 (2015)
39. Daghooghi, T., Soroosh, M., Ansari-Asl, K.: A novel proposal for all-optical decoder based on photonic crystals. Photonic Netw. Commun. **35**(2017), 335–341 (2017)
40. Mehdizadeh, F., Soroosh, M., Alipour-Banaei, H.: A novel proposal for optical decoder switch based on photonic crystal ring resonators. Opt. Quantum Electron. **48**(2015), 20 (2015)
41. Alipour-Banaei, H., Rabati, M.G., Abdollahzadeh-Badelbou, P., Mehdizadeh, F.: Effect of self-collimated beams on the operation of photonic crystal decoders. J. Electromagn. Waves Appl. **30**, 1440–1448 (2016)
42. Mehdizadeh, F., Alipour-banaei, H., Serajmohammadi, S.: Study the role of non-linear resonant cavities in photonic crystal-based decoder switches. J. Mod. Opt. **0340**, 1–9 (2017)
43. Moniem, T.A.: All optical active high decoder using integrated 2D square lattice photonic crystals. J. Mod. Opt. **62**, 1643–1649 (2015)
44. Gholamnejad, S., Zavvari, M.: Design and analysis of all-optical 4–2 binary encoder based on photonic crystal. Opt. Quantum Electron. **49**, 302 (2017)
45. Mehdizadeh, F., Soroosh, M., Alipour-Banaei, H.: Proposal for 4-to-2 optical encoder based on photonic crystals. IET Optoelectron. **11**, 29–35 (2017)
46. Moniem, T.A.: All-optical digital 4×2 encoder based on 2D photonic crystal ring resonators. J. Mod. Opt. **63**, 735–741 (2016)
47. Yang, Y.P., Lin, K.C., Yang, I.C., Lee, K.Y., Lee, W.Y., Tsai, Y.T.: All-optical photonic-crystal encoder capable of operating

at multiple wavelengths. Opt. Int. J. Light Electron Opt. **142**, 354–359 (2017)
48. Ouahab, I., Rafah, : A novel all optical 4×2 encoder switch based on photonic crystal ring resonators. Opt. Int. J. Light Electron Opt. **137**, 134–143 (2016)
49. Mehdizadeh, F., Soroosh, M., Alipour-Banaei, H., Farshidi, E.: A novel proposal for all optical analog-to-digital converter based on photonic crystal structures. IEEE Photonics J. **9**, 1–11 (2017a)
50. Mehdizadeh, F., Soroosh, M., Alipour-Banaei, H., Farshidi, E.: All optical 2-bit analog to digital converter using photonic crystal based cavities. Opt. Quantum Electron. **49**, 38 (2017b)
51. Tavousi, A., Mansouri-Birjandi, M.A., Saffari, M.: Successive approximation-like 4-bit full-optical analog-to-digital converter based on Kerr-like nonlinear photonic crystal ring resonators. Phys. E Low-Dimensional Syst. Nanostructures. **32**, 34–40 (2016)
52. Tavousi, A., Mansouri-Birjandi, M.A.: Optical-analog-to-digital conversion based on successive-like approximations in octagonal-shape photonic crystal ring resonators. Superlattices Microstruct. **23**, 76–83 (2017)
53. Youssefi, B., Moravvej-Farshi, M.K., Granpayeh, N.: Two bit all-optical analog-to-digital converter based on nonlinear Kerr effect in 2D photonic crystals. Opt. Commun. **285**, 3228–3233 (2012)
54. Miao, B., Chen, C., Sharkway, A., Shi, S., Prather, D.W.: Two bit optical analog-to-digital converter based on photonic crystals. Opt. Express. **14**(2006), 7966 (2006)
55. Myers, H.P.: Introductory Solid State Physics. Taylor & Francis, UK (2002)
56. Johnson, S., Joannopoulos, J.: Block-iterative frequency-domain methods for Maxwell's equations in a planewave basis. Opt. Express **8**, 173 (2001)
57. Ramaswami, R., K, Sivarajan, and G. Sasaki, : Optical networks: a practical perspective, 3rd edn.. Morgan Kaufmann, USA (2009)
58. Ogusu, K., Yamasaki, J., Maeda, Sh.: Linear and nonlinear optical properties of Ag-As-Se chalcogenide glasses for all-optical switching. Opt. Lett. **29**, 265–267 (2004)
59. Petrenko, A.D.: Nonlinear Kerr effect in magnetic crystals. Phys. Solid State. **41**, 591–594 (1999)
60. Li, C.: Nonlinear Optics: Principles and Applications. Springer, Heidelberg (2017)
61. Sullivan, D.M.: Electromagnetic simulation using the FDTD method. IEEE Press, USA (2000)
62. Werneck, M. M. M., Allil, R. C. S. B., De Nazaré, F. V. B. (2017) Fiber Bragg gratings: theory, fabrication, and applications. SPIE-The International Society for Optical Engineering.
63. Lowell, D., Hassan, S., Sale, O., Adewole, M., Hurley, N., Philipose, U., Chen, B., Lin, Y.: Holographic fabrication of graded photonic super-quasi-crystals with multiple-level gradients. Appl. Opt. **57**, 6598–6604 (2018)
64. Pang, L., Nakagawa, W., Fainman, Y.: Fabrication of two-dimensional photonic crystals with controlled defects by use of multiple exposures and direct write. Appl. Opt. **42**(2003), 5450–5456 (2003)
65. Campbell, M., Sharp, D.N., Harrison, M.T., Denning, R.G., Turberfield, A.J.: Fabrication of photonic crystals for the visible spectrum by holographic lithography. Nature **404**, 53–56 (2000)
66. Lowell, D., Hassan, S., Adewole, M., Philipose, U., Chen, B., Lin, Y.: Holographic fabrication of graded photonic super-crystals using an integrated spatial light modulator and reflective optical element laser projection system. Appl. Opt. **56**, 9888–9891 (2017)
67. Liu, Y., Liu, S., Zhang, X.: Fabrication of three-dimensional photonic crystals with two-beam holographic lithography. Appl. Opt. **45**, 480–483 (2006)
68. Ku, H.M., Huang, C.Y., Chao, S.: Fabrication of three-dimensional autocloned photonic crystal on sapphire substrate. Appl. Opt. **50**, C1–C4 (2011)
69. Schueller, O.J.A., Whitesides, G.M., Rogers, J.A., Meier, M., Dodabalapur, A.: Fabrication of photonic crystal lasers by nanomolding of solgel glasses. Appl. Opt. **38**, 5799–5802 (1999)
70. Chen, J.H., Huang, Y.T., Yang, Y.L., Lu, M.F., Shieh, J.M.: Design, fabrication, and characterization of Si-based ARROW photonic crystal bend waveguides and power splitters. Appl. Opt. **51**, 5876–5884 (2012)
71. Cui, L., Zhang, Y., Wang, J., Ren, Y., Song, Y., Jiang, L.: Ultrafast fabrication of colloidal photonic crystals by spray coating. Macromol. Rapid Commun. **30**, 598–603 (2009)
72. Freymann, G.V., Kitaev, V., Lotschz, B.V., Ozin, G.A.: Bottom-up assembly of photonic crystals. Chem Soc Rev. **42**, 2528–2554 (2012)

M. J. Maleki received his B.S. and M.S. degrees in Electronic Engineering from Islamic Azad University of Borujerd and Lorestan university, respectively. His fields of interests are all-optical devices based on photonic crystals.

A. Mir received the Ph.D. degree in electronic engineering from Tarbiat Modares University at Tehran in 2009. He is an associate professor of electronics in Lorestan University, Iran. His research interests are in modeling and simulation of photonic and optoelectronic devices.

M. Soroosh received the B.Eng. degree from the Isfahan University of Technology at Isfahan in 2000 and M.S. and Ph.D. degrees from Tarbiat Modares University at Tehran in 2003 and 2009, respectively, all in electronics. He joined the Iran Telecommunication Research Center, Tehran, in 2003 where he was a researcher at optical communication group. Currently, he is an associate professor of electronics in Shahid Chamran University of Ahvaz, Iran. His research interests are in modeling and simulation of photonic and optoelectronic devices.